

# Research Article

# Sacrificial-Layer Technique Fabrication and Characterization of Membrane Pneumatic Actuators for Flow Control in Microfluidics – Reproducibility Assessment

Siwapol Charykaew, Gridsada Phanomchoeng and Werayut Srituravanich Department of Mechanical Engineering, Faculty of Engineering, Chulalongkorn University, Bangkok, Thailand

# Thammawit Suwannaphan

Department of Mechanical Engineering Technology, College of Industrial Technology (CIT), King Mongkut's University of Technology North Bangkok, Bangkok, Thailand

#### Alongkorn Pimpin\*

Department of Mechanical Engineering, Faculty of Engineering, Chulalongkorn University, Bangkok, Thailand Micro/Nano Electromechanical Integrated Device Research Unit, Faculty of Engineering, Chulalongkorn University, Bangkok, Thailand

\* Corresponding author. E-mail: alongkorn.p@chula.ac.th DOI: 10.14416/j.asep.2025.11.004 Received: 9 June 2025; Revised: 20 August 2025; Accepted: 8 September 2025; Published online: 13 November 2025 © 2025 King Mongkut's University of Technology North Bangkok. All Rights Reserved.

#### **Abstract**

Ensuring the fabrication reproducibility of pneumatic actuators for a flow control in microfluidics is essential for their practical application. The actuator consists of a two-layered structure, including a control layer and a thin membrane. This study introduces a novel fabrication method that achieves uniform Polydimethylsiloxane (PDMS) membrane thickness and simplifies production using a polyvinyl alcohol (PVA) sacrificial layer and corona discharge bonding. Actuators with membrane diameters of 1,500, 2,000, and 2,500  $\mu$ m were successfully fabricated and analyzed. Experimental results indicate that membrane deflection increases with both applied pressure and membrane size. In this work, displacement variability was assessed to evaluate reproducibility. The investigation revealed consistent performance for actuators with membranes larger than 2,000  $\mu$ m, while smaller membranes exhibited greater deviation, suggesting the need for further process optimization. Overall, the fabricated microactuators demonstrate strong potential for reliable flow control in microfluidic systems.

Keywords: Microfluidics, Pneumatic actuator, Sacrificial layer, Soft lithography, Thin membrane

#### 1 Introduction

Microfluidic systems have gained significant attention over the past few decades due to their potential to revolutionize biological analysis, medical diagnostics, and chemical processing. These systems enable precise manipulation of very small liquid volumes within microchannels, thereby reducing sample consumption, minimizing reagent usage, improving analysis efficiency, and lowering operational costs. One of the most prominent applications of microfluidic systems is the Lab-on-a-Chip (LOC) platform, which integrates multiple biochemical and analytical processes onto a single

microchip [1]–[3]. This miniaturized platform facilitates rapid and accurate diagnostics compared to conventional laboratory methods. Further advancements have enabled LOC devices to incorporate multiple sequential steps, including sample preparation, mixing, separation, and detection, into a single compact system, significantly enhancing biochemical assay efficiency [4]–[7].

Despite these advances, precise and dynamically adjustable flow-rate control remains a major challenge in microfluidic biological analysis. Many applications demand drastically different flow conditions; for instance, cell separation typically operates at high flow rates (~1 mL/min), whereas cell trapping and



capture require very low flow rates (~0.1 mL/h) [5], [7]. Integrating both functions in a single microfluidic chip requires flow control elements that can adapt to such extreme variations without compromising system stability. External pressure-driven pumps, such as syringe pumps and peristaltic pumps, are widely used but have inherent limitations, including bulky size, slower response time, and limited adaptability. To address these issues, various miniature flow control components, particularly microvalves driven by microactuators, have been integrated into microfluidic systems [8]–[10]. Several actuation mechanisms have been explored: 1) electroactive actuators, such as electroactive polymers (EAPs), deform membranes upon voltage application and offer fast, tuneable control but may cause electrochemical interference with biological samples [11]–[13]; 2) thermal actuators, such as bimetallic designs, modulate flow through thermally induced mechanical deformation but risk localized heating that could harm cells or biochemical reactions [14]; and 3) magnetic actuators, which manipulate ferro-fluidic elements or flexible membranes using external magnetic fields, enabling non-contact control but requiring complex and bulky fieldgeneration systems [11], [15]. Therefore, pneumatic actuators have emerged as a promising alternative [9], [16]–[19], operating by applying controlled air pressure to flexible membranes or elastomeric structures, thus avoiding electrical or thermal perturbations while enabling continuous and dynamic flow regulation. Polydimethylsiloxane (PDMS) is the preferred material for pneumatic membranes due to its biocompatibility, elasticity, and ease of fabrication [11]–[13], [17], [18], [20]-[27], and fabrication methods such as corona discharge bonding or plasma bonding are employed to ensure robust sealing [22], [23]. However, the fabrication and bonding of thin, deformable membranes remain challenging. Among various techniques, sacrificiallayer-based fabrication that allows membrane release without harsh chemicals [27]–[29], with water-soluble layers, would be a good choice. However, some materials, such as polycarbonate membranes [28]-[29], are rigid, thus complicating subsequent multilayer assembly processes.

To address these limitations, this study presents a novel fabrication approach that improves the manufacturability and reliability of multi-layer pneumatic microactuators for microfluidic applications. The developed actuator features a three-layer PDMS structure: a control layer for air pressure regulation, a fluidic layer for liquid transport, and a thin deformable

membrane that dynamically modulates flow in response to pneumatic pressure. An optimized polyvinyl alcohol (PVA) sacrificial-layer technique combined with corona discharge bonding is employed to achieve uniform membrane thickness, strong interlayer adhesion, and reproducible fabrication suitable for scalable production. The key contributions of this study include the enhanced fabrication process by utilizing improved soft lithography with an optimized sacrificial layer to ensure consistent, reproducible membrane formation and precise actuation. The scalable design supports mass production for microfluidic applications. Also, evaluation of the performance by developing an experimental setup to characterize membrane deflection under varying pressures to ensure the actuator meets the demands of research work. These advancements enhance the actuator's practicality and precision, making it a viable solution for various microfluidic applications.

#### 2 Materials and Methods

#### 2.1 Structures of the actuator

The pneumatic actuator developed in this study consists of four key components as shown in Figure 1(a) and (b). The control layer serves as the main structural component that houses the microfluidic channels, facilitating controlled air pressure distribution. The thin membrane is a flexible component that deforms in response to applied pneumatic pressure, enabling dynamic fluid control within the microchannels. The connection port is an interface between the actuator and the external pneumatic system, allowing efficient pressure regulation, while the air tube is used to deliver compressed air to the system.

#### 2.2 Fabrication processes

All structures are made of PDMS. The control layer and connection ports are fabricated using standard soft lithography, while the thin membrane is fabricated using a sacrificial layer-assisted method to ensure uniform thickness and mechanical integrity. In addition, the air tubing is integrated using commercially available standard components, ensuring ease of assembly. To assemble these layers, corona discharge bonding is employed to ensure robust adhesion between the PDMS layers. The final actuator is integrated with external pneumatic tubing using needle or tube insertion. After assembly, the actuator is tested for leakage by



connecting it to the air compressor unit. The fabrication process is summarized in Figure 2(a).

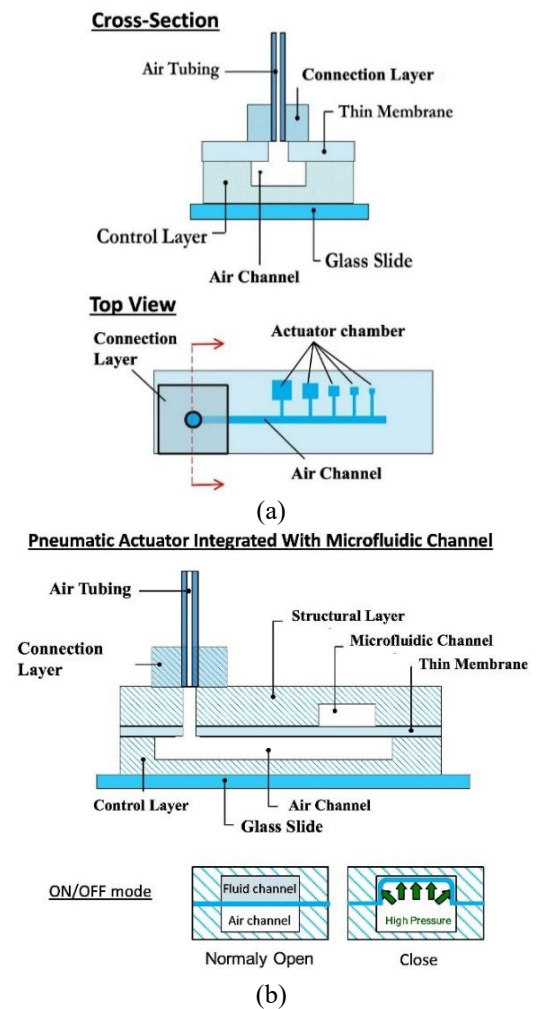
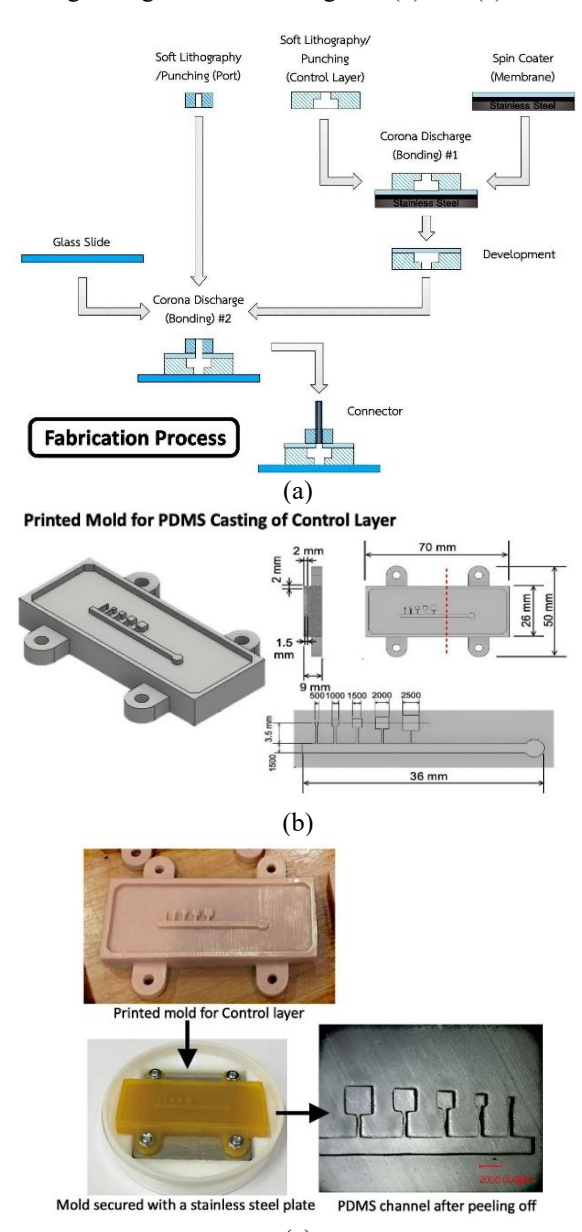


Figure 1: Structures of the pneumatic actuator (a) Cross-section of the actuator, (b) The pneumatic actuator and microfluidic channel.

For the control layer and connection port, the molds to cast PDMS were fabricated using stereolithography (SLA) 3D printing due to its ability to rapidly produce complex microfluidic patterns at a lower cost. However, surface roughness from the 3D-printed mold can impact the quality of the final PDMS microchannel, necessitating additional surface finishing treatments. To improve mold reliability, a prototype mold was developed with an enhanced thickness and structural reinforcement to reduce warping during the curing process. Key modifications include:

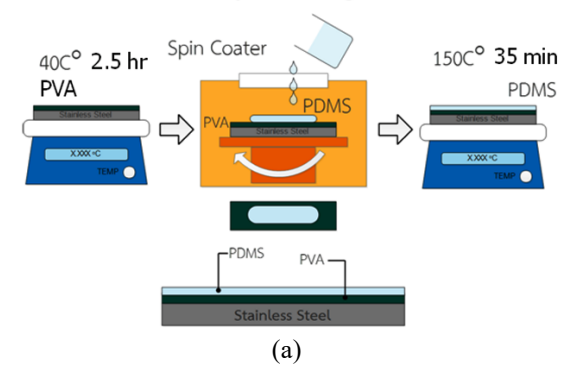
- Increasing the mold thickness to enhance durability.
- Orienting the 3D print layers along the vertical direction to achieve a smoother surface finish.
- Implementing stainless steel plates with screws and bolts to fix the mold in place, minimizing deformation during curing, as shown in Figure 2(b) and (c).



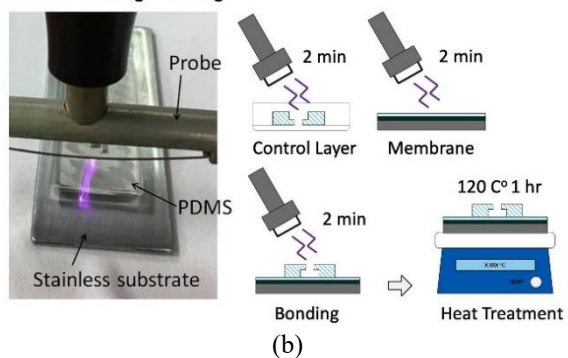
**Figure 2**: The fabrication of a pneumatic actuator: (a) Process flow, (b) CAD image of the mold with dimensions, (c) 3D-printed mold with screws and bolts and PDMS microchannel.



#### **PDMS Membrane Layer Forming**



#### Corona Discharge Bonding

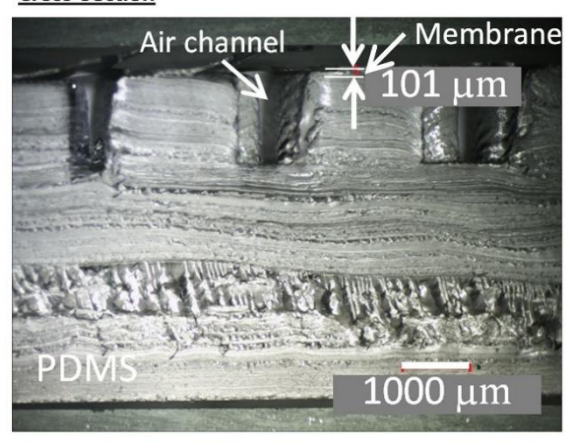


# Connection layer and Tubing hole Glass slide PDMS membrane



(c)

#### **Cross-Section**



(d)

Figure 3: Membrane fabrication and bonding processes (a) Spin-Coating PDMS membrane and heat treatment, (b) Corona discharge treatment, (c) The completed pneumatic actuator: after bonding the control layer from the mold with the thin membrane, (d) Cross-section of the air channel and thin PDMS membrane.

This optimized mold design supports the fabrication of three different actuator sizes ( $500-2,500~\mu m$ ), allowing for versatility in applications. The highlight of the fabrication process is the sacrificial layer-assisted thin film deposition for the thin membrane. The thin membrane is fabricated on a polyvinyl alcohol (PVA) sacrificial layer, which facilitates structural integrity before bonding, as shown in Figure 3(a).

Firstly, a stainless steel substrate is coated with PVA and heated at 40 °C for 2.5 h to form a uniform dissolvable layer. Then, a two-step spin-coating process consisting of step 1: 500 rpm for 5 s for uniform spreading, and step 2: 3000 rpm for 30 s to achieve the desired thin-film thickness ( $100 \pm 3.5 \, \mu m$ ) is employed to apply PDMS on the PVA layer. This spinning process ensures high uniformity across the membrane. The coated membrane is thermally cured at 150 °C for 35 min for structural stability. After that, the thin membrane is stored in the humidity-controlled environment to prevent premature degradation before integration.

The final step involves integrating the control layer, thin membrane, and connection ports into a functional pneumatic actuator. This is achieved through corona discharge bonding, a rapid and cost-effective adhesion method as shown in Figure 3(b). Firstly, the control layer and thin membrane undergo



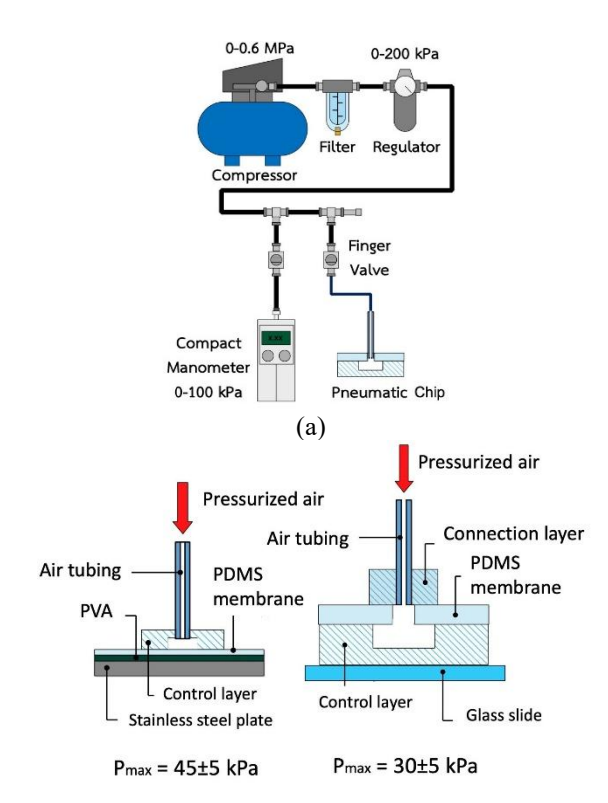
corona discharge treatment for 2 min to enhance surface adhesion. The activated surfaces are carefully aligned and pressed together, eliminating trapped air bubbles. The assembled structure is placed in an oven at 120 °C for 1 hour to strengthen adhesion. To release the PDMS structure from the stainless steel substrate, the assembled structure was indirectly placed in an ultrasonic sonicator bath for 4 h before the PDMS structure was carefully peeled off in a 120 °C water bath. After drying, the PDMS structure was bonded to a glass slide, and, at the end, the connecting ports were bonded. Figure 3(c) and (d) show the completed device on the glass slide and the air channel's cross-section, respectively. We observed that the uniformity of the cross-section was very good.

# 2.3 Test strategy

The experiment aims to evaluate the membrane deflection characteristics of the fabricated pneumatic actuators to assess their reproducibility and structural integrity under controlled pressure conditions. The ability to reproducibly manufacture actuators that respond predictably to applied pressure is crucial for their practical implementation. Five samples of the same system were fabricated and tested to achieve this. The study focuses on actuator sizes of 1,500, 2,000, and 2,500 µm, selected based on their potential to produce effective actuation while maintaining fabrication consistency. The actuators were subjected to stepwise pressure increments to measure deflection, and the results were analyzed to determine actuation characteristics and fabrication reproducibility.

#### 2.4 Experimental setup for testing

A controlled pneumatic system and an optical measurement setup were designed to ensure precise and repeatable deflection measurements. The actuators were securely mounted on glass slides using corona discharge bonding to prevent unwanted displacement during testing. To apply pressure, a regulated air control system was connected to the actuator, allowing for fine adjustments in air pressure from 0 to 200 kPa. The experimental setup is shown in Figure 4(a). The bonding strength was tested for two cases, including the strength between PDMS-PDMS membrane and PDMS-PDMS membrane and PDMS-PDMS membrane-PDMS bonding, as shown in Figure 4(b). It was found that the maximum pressure that is possible was  $45 \pm 5$  kPa and  $30 \pm 5$  kPa, respectively.



Tests for the strength of bonding by stepping the pressure of 5 kPa and holding for 5 min

(b)

**Figure 4**: The experimental setup (a) Schematic of the pressurized air controller, (b) Bonding strength tests.

To ensure compatibility with the custom-designed 3D-printed fixture, each actuator sample was carefully trimmed to the appropriate dimensions, allowing it to fit securely within the fixture's designated slots. This ensured stable positioning during the experiment while maintaining optical accessibility. The trimmed samples were then aligned and positioned under the microscope, ensuring that both top and side views of the membrane were clearly visible. A 45° angled mirror was placed adjacent to the actuator, allowing for side-view imaging of the membrane deflection without obstructing the optical path, as shown in Figure 5.

Membrane deflection was captured using the stereomicroscope positioned to observe both the top and side views of the actuator. A 3,000  $\mu$ m diameter metal ball was placed within the imaging field as a distance reference and used for adjusting the orientation of the actuators and mirror to ensure the precision of experiments.



The bias uncertainty for the measuring system is mainly due to the camera's resolution, which is approximately 20  $\mu m$ . With the calibrations using the metal ball, the bias uncertainty to measure the distance of this setup, including the improper orientation of the mirror and actuators, was found to be less than 50  $\mu m$  or approximately 2% of the metal ball's diameter. Therefore, two percent of the measured distance is expected to be the bias uncertainty of this experimental setup when the measured distance is longer than the camera's resolution of 20  $\mu m$ .

## 2.5 Test procedure

The actuators were tested under static and dynamic pressure conditions to characterize their deformation behavior. The applied pressure was gradually increased in increments of 5 kPa, ranging from 0 to 25

kPa, while the membrane deflection was recorded at each step. The stereomicroscope captured high-resolution images, and the displacement of the membrane was analyzed using image processing software. The deflection trends were analyzed to determine actuation efficiency, and variability across five fabricated samples was examined.

For dynamic tests, the actuators were driven at 1, 5, and 20 Hz (duty cycle of 50%), controlled by a directional solenoid valve installed at the inlet of the tested actuators, when the pressurized air was set at 25 kPa. In addition, to check the setup installation's repeatability, the variability of the measured displacement of each actuator in each sample was investigated by repeatedly uninstalling and reinstalling the sample into the test setup. The displacement deviation of the same actuator for each installation was approximately lower than 5% for all cases.

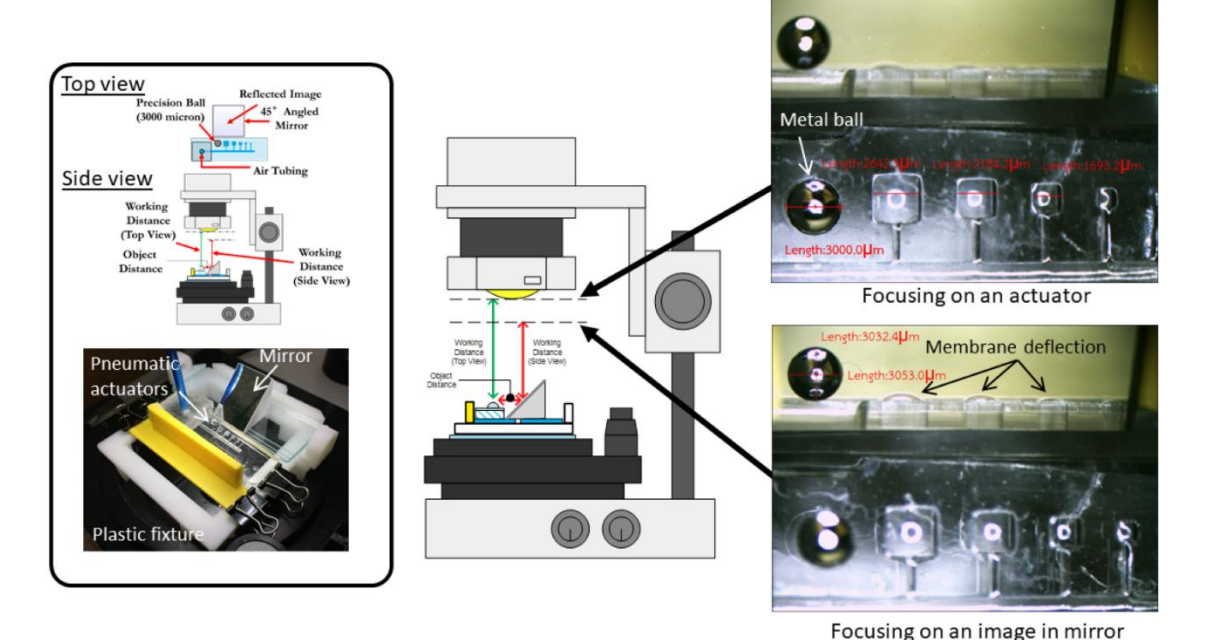


**Figure 5**: Images of the setup of the pneumatic actuators on the stereomicroscope.

# 3 Results and Discussion

## 3.1 Effects of the fabrication processes

The deflection of the membrane was recorded at 0, 15, 20, and 25 kPa, and the displacements at each pressure were calculated by comparing the image with that at 0 kPa. Averaged displacements for all five fabricated samples are presented in Figure 6. The averaged

displacements of each sample were repeatedly measured in three sets at each pressure, and there were three measurements in each set. The variability of each set was lower than 5% of the averaged values, except in batch no. 4. In this case, the variability reached 10–15% in some tests.

The experimental results demonstrate a direct correlation between membrane size and deflection magnitude. Larger actuators exhibited greater deflection



under equivalent pressure conditions. In addition, for a certain actuator, the deflection magnitude increases about 30–40% when the applied pressure increases from 15 to 25 kPa.

However, the deviation of displacements was found among these tested samples. The tendency is that the deviation was higher at lower pressure levels and smaller actuators. The former one should be the effects of the measurement system's bias uncertainty, while the latter one should be the effects of manufacturing processes.

For example, at the pressure of 25 kPa, the averaged displacements with their standard deviation for each actuator size from all five samples were:

- 1,500  $\mu$ m: 237  $\pm$  37  $\mu$ m
- 2,000  $\mu$ m: 354  $\pm$  7  $\mu$ m
- $2,500 \mu m$ :  $491 \pm 22 \mu m$

The standard deviations of about 5–15% of the averaged value indicate the inconsistent mechanical properties among actuators with the same parameters. Notably, higher variability was observed at 1,500 μm actuators, about 37 µm (or 15% of the averaged value), which is much higher than the experiment's bias uncertainty. At larger scales, the deviations became smaller, and at the sizes of 2,000 and 2,500 µm, the variability reduced and was only 2 and 4.5% of the averaged displacement, respectively. The results implied that the deviations of deflection, which might be results of the variation of the actuator's properties, mainly occurred in the fabrication process, significantly increased for smaller scales. It is attributed to higher sensitivity to the fabrication processes at smaller actuator sizes, and in these experiments, the characteristics of the actuators with a membrane size smaller than 2,000 µm should be carefully considered.

According to the results, a suitable operation of the developed actuators should be ON/OFF mode since the ability to control the displacement was not precise. They varied between each actuator sample with the same parameters. The concept to utilize the pneumatic actuator is simple by applying a certain high pressure to close the fluidic channel, not allowing liquid to flow through, as shown in Figure 1(b).

From dynamic tests at 1, 5 and 20 Hz, it was found that displacements reduced significantly at 5 Hz. In addition, the displacements became very small and could not be measured at 20 Hz. This is a limitation of the entire system, including the tubing connecting the compressor and devices. Comparing the displacements measured in two experiments (static

test and dynamic test at 1 Hz), the deflections changed a little. It suggests that the system responds well at the driving frequency of 1 Hz. Therefore, the developed actuators would be suitable for the operation in the ON/OFF mode at a driving frequency lower than 1 Hz.

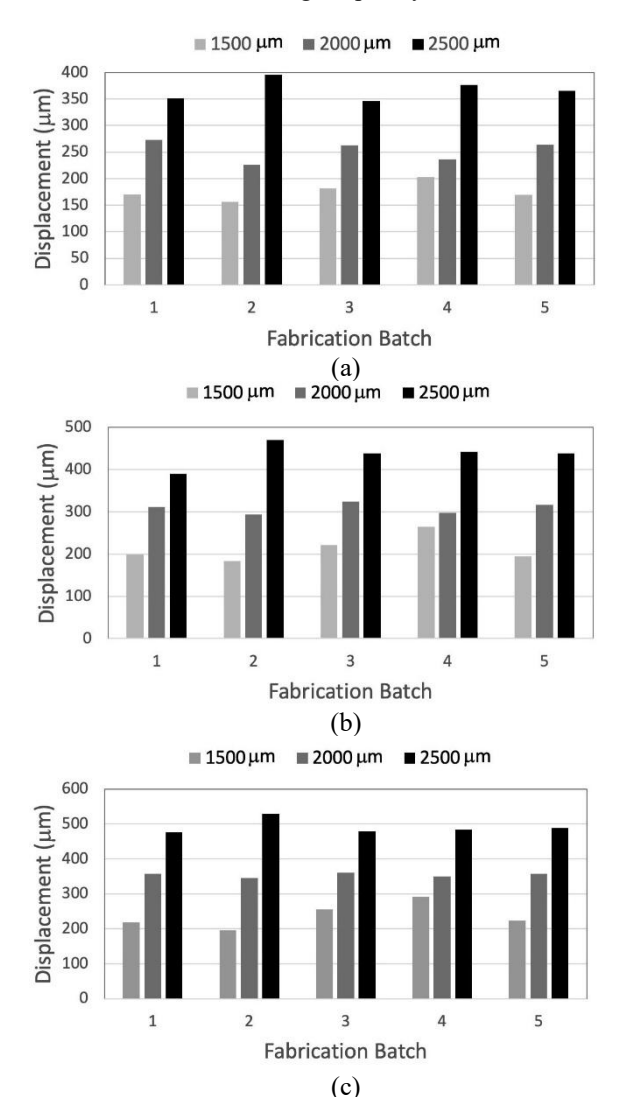


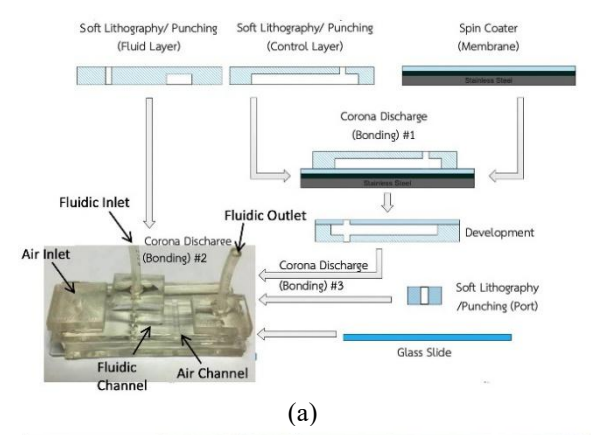
**Figure 6**: Membrane deflection for 1,500, 2,000, and 2,500 μm pneumatic actuators (a) Pressurized air at 15, (b) 20, (c) 25 kPa.

# 3.2 Durability tests

The actuators were tested for their durability when actuated at 5 Hz at a pressure of 25 kPa for 50,000 cycles. The static deflections were measured again using the same procedure in the previous section, after actuation for 25,000 and 50,000 cycles. It was found



that the displacements tended to decrease slightly after 50,000 cycle actuation. From our experiments, the displacements were less than 5% changed, and the results indicated that the actuators could return to their original shape after pressure release with negligible residual deformation.



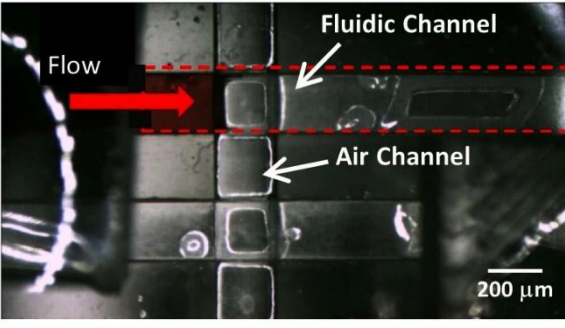


**Figure 7**: Integration of PDMS pneumatic microactuators and fluidic channels (a) Process flow, (b) Flow at the flow rate of 0.5 mL/min stopped after actuation at the pressure of 35 kPa.

(b)

# 3.3 Microfluidic applications

The developed pneumatic microactuators were integrated with the microfluidic channel to demonstrate their ability to control the flow. All devices were made of PDMS by bonding all layers together using the corona discharge technique. Figure 7 shows the fabrication process as the fluidic layer was added to the PDMS membrane previously bonded to the control layer. In experiments, the air channel was designed as  $2,000 \times 2,000$  µm while the fluidic microchannel was designed as  $2,000 \times 300$  µm. When they were perpendicularly overlaid, the square PDMS membrane with a size of 2,000 µm was formed. Two

liquid flow rates were set at 0.5 and 1.0 mL/min by a syringe pump while the pressurized air was 5 kPa stepwise increased. We have found that at 0.5 mL/min or an average flow velocity of 13.8 mm/s, the pneumatic actuator could completely stop this high-speed flow when applying the pressure of 25–35 kPa. The gauge pressure of the liquid flow at the actuator site is approximated to be about 500 Pa when the pneumatic actuator is not actuated and the microchannel is fully opened. However, the gauge pressure could significantly increase when the pneumatic actuator almost completely closes the microchannel. From the experiments, we found that the actuator could not completely stop the flow at a faster speed of 1.0 mL/min.

#### 3.4 Performance comparison

We have compared our results with past work [17], [24]–[26], and the performance comparison is shown in Table 1. Although the actuators are not exactly in the same dimensions, the deflection measurement in this current work shows comparable results with those in the past work. We have found that, among the PDMS membrane sizes of 0.5–4 mm with the approximated thickness of 100  $\mu$ m, the deflection displacement is about 0.15–0.2 times of the membrane size when the air pressure of 10–100 kPa is applied, and the feasible driving frequency is about 1 Hz.

**Table 1:** Performance comparison of PDMS membrane pneumatic actuators.

Authors	Dimensions	Displacement	Frequency
Qian et al.	4 mm (circle) with	600 µm at 2.5	N/A
[24]	approx. 100 μm thickness	kPa pressure	
Yuan et al. [25]	500 μm (circle) with approx. 70-80 μm thickness	90 μm at 60 kPa pressure	N/A
Nanaware et al. [26]	2x4 mm (rectangle) with approx. 350 μm thickness	N/A (to control 25-100 µL/min flow rate with max. 96 kPa pressure)	N/A
Liu et al. [17]	Approx. 300x500 μm (rectangle) with approx. 40 μm thickness	100 μm at 70 kPa pressure	1 Hz

The advantage of the use of a flexible membrane is its conformability to a channel's surface. When applying an adequately high pressure, it can completely close the flow channel in microfluidic applications. However, the similar membrane



structures and their fabrication processes could be applied for various applications such as a pneumatically-driven soft gripper for robotics [19], a pressure sensor with a flexible sensing unit [27], and a thermal sensor that requires an insulating air cavity [30]. Only the shape and thickness of the membrane must be redesigned to suit the desired applications.

#### 4 Conclusions

This study successfully developed and characterized a pneumatic PDMS actuator for microfluidic flow control using a soft lithography process combined with an optimized PVA sacrificial-layer technique and corona discharge bonding. The proposed fabrication method enabled the formation of uniform, reproducible membranes and achieved high bonding strength between PDMS layers. Experimental results demonstrated that the actuator maintained mechanical integrity under controlled pressure conditions and was capable of reliably modulating flow within microchannels. For 2,000 µm square membranes integrated into 2,000 × 300 µm microchannels, ON/OFF flow control at a rate of 0.5 mL/min was achieved using pressurized air in the range of 25-35 kPa. Fabrication reproducibility was high for large membranes (>2,000 μm), while smaller membranes exhibited greater deviations, likely due to fabrication tolerances.

However, certain limitations remain. The residual PVA layer removal process is critical for ensuring bonding quality, and any incomplete removal can reduce long-term reliability. Furthermore, the observed variation in mechanical performance for small membrane sizes highlights the need for process refinement at micro-scales. Future work will focus on optimizing the sacrificial layer removal for submillimeter membranes, improving bonding techniques for complex multi-layer assemblies, and exploring integration with more advanced microfluidic platforms for biomedical applications. Challenges such as scaling the fabrication for mass production while maintaining uniformity and ensuring actuator performance under continuous long-term operation will also be addressed in subsequent studies.

#### Acknowledgments

This research was financially supported by the Thailand Science Research and Innovation Fund, Chulalongkorn University (RCU-68-026-2100-001).

#### **Author Contributions**

S.C.: research design, methodology, data curation, data analysis; G.P.: writing an original draft; W.S.: research design, methodology; T.S.: writing—reviewing and editing, project administration; A.P.: conceptualization, research design, methodology, data analysis, investigation, funding acquisition, writing—reviewing and editing. All authors have read and agreed to the published version of the manuscript.

#### **Conflicts of Interest**

The authors declare no conflict of interest.

#### References

- [1] J. M. Ayuso, M. Virumbrales-Muñoz, J. M. Lang, and D. J. Beebe, "A role for microfluidic systems in precision medicine," *Nature Communications*, vol. 13, no. 1, 2022, Art. no. 3086.
- [2] R. Driver and S. Mishra, "Organ-On-A-Chip technology: An in-depth review of recent advancements and future of whole body-on-chip," *Biochip Journal*, vol. 17, pp. 1–23, 2023.
- [3] A. Valizadeh and A. Y. Khosroushahi, "Single-cell analysis based on Lab on Chip fluidic system," *Analytical Methods*, vol. 7, no. 20, pp. 8524–8533, 2015.
- [4] U. A. Gurkan et al., "Next generation microfluidics: Fulfilling the promise of lab-on-a-chip technologies," *Lab on a Chip*, vol. 24, no. 7, pp. 1867–1874, 2024.
- [5] P. Panuska et al., "Advanced microfluidic platform for tumor spheroid formation and cultivation fabricated from OSTE+ polymer," *Biochip Journal*, vol. 18, pp. 393–409, 2024.
- [6] C. D. Chin, V. Linder, and S.K. Sia, "Lab-on-achip devices for global health: Past studies and future opportunities," *Lab on a Chip*, vol. 7, no. 1, pp. 41–57, 2007.
- [7] T. Wongpakham et al., "Development of pyramidal microwells for enhanced cell spheroid formation in a cell-on-chip microfluidic system for cardiac differentiation of mouse embryonic stem cells," Cells, vol. 13, no. 24, p. 2132, 2024.
- [8] D. Popa, "Microactuators," in *Encyclopedia of Microfluidics and Nanofluidics*, 2008, pp. 1000–1003.



- [9] W. O. Kwang and H. A. Chong, "A review of microvalves," *Journal of Micromechanics and Microengineering*, vol. 16, no. 5, 2006, Art. no. R13.
- [10] M. R. A. Fuaad, M. N. Hasan, M. I. A. Asri, and M. S. M. Ali, "Microactuators technologies for biomedical applications," *Microsystem Technologies*, vol. 29, no. 7, pp. 953–984, 2023.
- [11] C. Y. Chen, C. H. Chen, T. Y. Tu, C. M. Lin, and A. M. Wo, "Electrical isolation and characteristics of permanent magnet-actuated valves for PDMS microfluidics," *Lab on a Chip*, vol. 11, no. 4, pp. 733–737, 2011.
- [12] J. D. Tice, T. A. Bassett, A. V. Desai, C. A. Apblett, and P. J. A. Kenis, "A monolithic poly(dimethylsiloxane) electrostatic actuator for controlling integrated pneumatic microsystems," *Sensors and Actuators A: Physical*, vol. 196, pp. 22–29, 2013.
- [13] A. V. Desai, J. D. Tice, C. A. Apblett, and P. J. A. Kenis, "Design considerations for electrostatic microvalves with applications in poly(dimethylsiloxane)based microfluidics," *Lab on a Chip*, vol. 12, no. 6, pp. 1078–1088, 2012.
- [14] K. Pitchaimani, B. C. Sapp, A. Winter, A. Gispanski, T. Nishida, and Z. H. Fan, "Manufacturable plastic microfluidic valves using thermal actuation," *Lab on a Chip*, vol. 9, no. 21, pp. 3082–3087, 2009.
- [15] J. Atencia, G. A. Cooksey, A. Jahn, J. M. Zook, W. N. Vreeland, and L. E. Locascio, "Magnetic connectors for microfluidic applications," *Lab* on a Chip, vol. 10, no. 2, pp. 246–249, 2010.
- [16] J. Casals-Terré et al., "Design, fabrication and characterization of an externally actuated ON/OFF microvalve," *Sensors and Actuators A: Physical*, vol. 147, no. 2, pp. 600–606, 2008.
- [17] X. Liu et al., "Theoretical and experimental studies of a PDMS pneumatic microactuator for microfluidic systems," *Energies*, vol. 15, no. 22, p. 8731, 2022.
- [18] X. Liu et al., "Microfluidics chips fabrication techniques comparison," *Scientific Reports*, vol. 14, 2024, Art. no. 28793.
- [19] H. G. Shin, W. K. Chung, and K. Kim, "Soft and flexible robot skin actuator using multilayer 3D pneumatic network," *Nature Communications*, vol. 16, 2025, Art. no. 5575.
- [20] J. C. McDonald and G. M. Whitesides, "Poly(dimethylsiloxane) as a material for fabricating microfluidic devices," Accounts of

- Chemical Research, vol. 35, no. 7, pp. 491–499, 2002.
- [21] K. Khanafer, A. Duprey, M. Schlicht, and R. Berguer, "Effects of strain rate, mixing ratio, and stress-strain definition on the mechanical behaviour of the polydimethylsiloxane (PDMS) material as related to its biological applications," *Biomedical Microdevices*, vol. 11, no. 2, pp. 503–508, 2008.
- [22] C. F. Chen and K. Wharton, "Characterization and failure mode analyses of air plasma oxidized PDMS-PDMS bonding by peel testing," *RSC Advances*, vol. 7, no. 3, pp. 1286–1289, 2017.
- [23] C. H. Chiou, T. Y. Yeh, and J. L. Lin, "Deformation analysis of a pneumatically activated polydimethylsiloxane (PDMS) membrane and potential micro-pump applications," *Micromachines*, vol. 6, no. 2, pp. 216–229, 2015.
- [24] X. Qian et al., "Characterizing the deformation of the polydimethylsiloxane (PDMS) membrane for microfluidic system through image processing," *Micromachines*, vol. 7, no. 5, p. 92, 2016.
- [25] Y. Yuan, Y. Yalikun, N. Ota, and Y. Tanaka, "Properly investigation of replaceable PDMS membrane as an actuator in microfluidic device," *Actuators*, vol. 7, no. 4, p. 68, 2018.
- [26] A. Nanaware et al., "Pneumatic controlled nanosieve for efficient capture and release of nanoparticles," *Journal of Vacuum Science & Technology B*, vol. 40, 2022, Art. no. 063002.
- [27] B. J. Koo et al., "Micromachined PVA (poly(vinyl alcohol)) sacrificial layer for facile and scalable demonstration of highly reproducible porous-type pressure sensor," ACS Applied Polymer Materials, vol. 6, pp. 11788–11797, 2024.
- [28] J. Hong, J. Gong, Q. Li, Z. Deng, and L. Gui, "A handy reversible bonding technology and its application on fabrication of an on-chip liquid metal micro-thermocouple," *Lab on a Chip*, vol. 21, pp. 4566–4573, 2021.
- [29] Z. Ye, Q. Li, R. Zhang, P. Zhang, and L. Gui, "Fabrication of a thin PDMS film with complex liquid metal electrodes embedded and its application as skin sensors," *RSC Advances*, vol. 12, pp. 8290–8299, 2022.
- [30] M. Li et al., "Fabrication and characterization of high-sensitivity, wide-range, and flexible MEMS thermal flow velocity sensors," *Microsystems & Nanoengineering*, vol. 10, 2024, Art. no. 102.